RSC Advances

ROYAL SOCIETY OF CHEMISTRY

www.rsc.org/advances

Table of Contents (TOC) Graphic

TiO_2@CdSe/CdS Core-Shell Hollow Nanospheres Solar Paint

*Xiang Zhang, Hongxia Sun,Xiyun Tao and Xingfu Zhou**

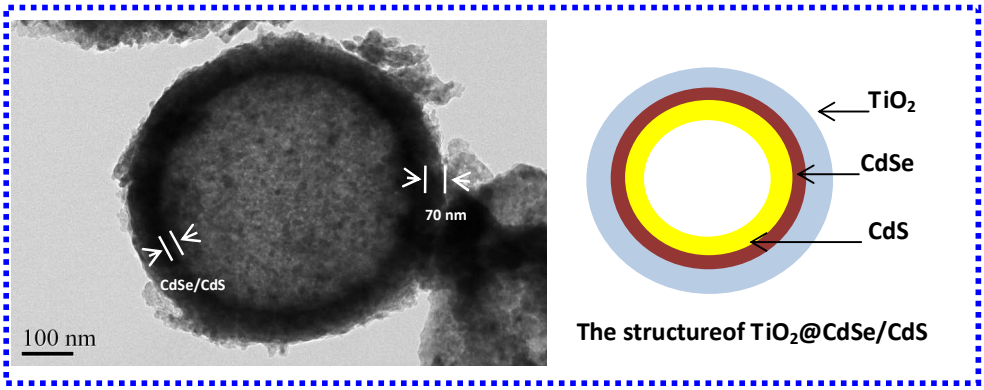

TiO_2@CdSe/CdS hollow Nanosphere solar paint were fabricated and directly applied in quantum dot sensitized solar cell. The reliable conversion efficiency of 0.79 with a current density of 6.6 mA/cm^2 was achieved.

Journal Name RSCPublishing

ARTICLE

TiO_2@CdSe/CdS Core-Shell Hollow Nanospheres Solar Paint

Cite this: DOI: 10.1039/x0xx00000x

*Xiang Zhang, Hongxia Sun, Xiyun Tao and Xingfu Zhou**

Received 00th January 2012,
Accepted 00th January 2012

DOI: 10.1039/x0xx00000x

www.rsc.org/

TiO_2@CdSe/CdS core-shell hollow nanospheres solar paint was successfully prepared via hard template and ion exchange method considering the match of their band gap. The outer layer of TiO_2 shell protects CdSe and CdS from decomposition and increases their stability. The diameters of the TiO_2@CdSe/CdS hollow nanospheres were uniformly around 600 nm with a shell thickness of 70 nm. The visible light absorption onset of TiO_2@CdSe/CdS hollow nanospheres is around 650 nm corresponding to a bandgap of 1.8 eV, showing a red-shift when compared with TiO_2/CdS. TiO_2@CdSe/CdS hollow nanospheres can be directly used as solar paint, the photoanode decorated by the solar paint performs a reliable photoelectric conversion efficiency of ~0.79% and current density of 6.6 mA/cm^2.

1. Introduction

There is a stringent global need for alternative, renewable energy sources for both economic and environmental reasons. One extremely attractive source of energy is the sun, which continuously transmits enormous quantities of light energy to earth. Can you imagine a kind of paint with simple brush can make the light energy into electricity?

Quantum dot sensitized solar cell (QDSSC) has attracted tremendous research interests because of its excellent properties, such as photostability, high molar extinction coefficients, size-dependent optical properties, low costs and little environmental impact.[1,2] It has also drawn significant attention as a feasible candidate for boosting the solar energy conversion efficiency owing to its theoretical maximum thermodynamic conversion efficiency as high as 44%[3]. The employment of QDs as a sensitizer in solar cells is mainly based on their tunable size-dependent properties, including multiple carrier generation (MEG), hot electron utilization and effective charge transfer[4,5]. Due to the small size of quantum dots and the broad absorption area, QDSSC could capture nearly the entire incident solar light in the visible region.

The photoanode of QDSSC is typically a sensitized nanocrystalline TiO_2 or ZnO film prepared by screen-print or doctor blade method, then sensitized by CdS, CdSe, PbS quantum dots. As we all know, sensitization is an important and essential process during the preparation of solar cell, which has a significant impact on the performance of the cell. Quantum dot sensitization method commonly use successive ion layer adsorption and reaction method (SILAR)[4,6,7],chemical bath deposition(CBD)[8, 9],spray pyrolysis deposition (SPD)[10-12], electro deposition (ED)[13, 14] and so on. No matter what kind of method, it is time-intensive, requiring multiple steps and a long time to complete the integrity of photoanode film deposition and annealing protocols in order to attain the best performing cells. There are many kinds of quantum dots such as CdS[15, 16], CdSe[17], InP[18], PbS[19, 20], PbSe[21] and InAs[22]. Plenty of research has been carried out to improve the performance of quantum dot-sensitized solar cells, one such example utilizes a PbS and P_{25} heterojunction is reported to exhibit a power conversion efficiency of 5.58 % by Hg^{2+} doping into PbS[19]. Quantum dot sensitized solar cell research usually employ CdS and CdSe as co-sensitizer, whose relative band edges are 2.25 eV and 1.7 eV[20, 23, 24] respectively, and the photoelectric conversion efficiency around 4~6[5, 25-30] is usually achieved. However, quantum dot used in QDSSC is usually unstable and lead to the decay of conversion efficiency in the air.

Taking into consideration of quantum dot stability and the Fermi level alignment, we synthesize a kind of core-shell hollow sphere nanostructure. The configuration of the TiO_2@CdSe/CdS hollow spheres (THS) is titanium dioxide in outer shell layer, CdSe in the middle layer, CdS in the inner layer, such a structure aim at injecting an excited electron from inner CdSe layer to outer TiO_2 layer and transferring a hole out of inner CdSe to electrolyte then conduct away. Further, we have prepared the energy level matching THS into the visible light responsive solar paint. As long as the obtained solar paint is simply brushed onto the surface of FTO, reliable photoelectric conversion efficiency of 0.79% with a current density of 6.6 mA/cm^2 was achieved.

2. Results and discussion

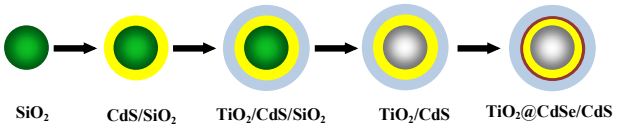

Fig.1. Schematic diagram of synthetic process of TiO_2@CdSe/CdS hollow spheres

The schematic diagram for the synthesis of TiO_2@CdSe/CdS hollow spheres (THS) is shown in **Fig.1**. The experiment was designed based on the case that the solubility product constant of CdS (~7.94×10^{-27}) is much larger than that of CdSe (~6.3×10^{-36}), this implies that the CdS layer can be used as sacrificial templates to further transform into more stable CdSe by anion exchange. Firstly, templates SiO_2 nanospheres were covered with CdS and TiO_2 in order to form TiO_2/CdS/SiO_2 core-shell spheres. Then, the SiO_2 cores were removed by hydrothermal treatment. Finally, the TiO_2/CdS double-shelled hollow spheres (DHS) were infiltrated in Selenium source of the aqueous solution for several hours to obtain TiO_2@CdSe/CdS hollow nanospheres.

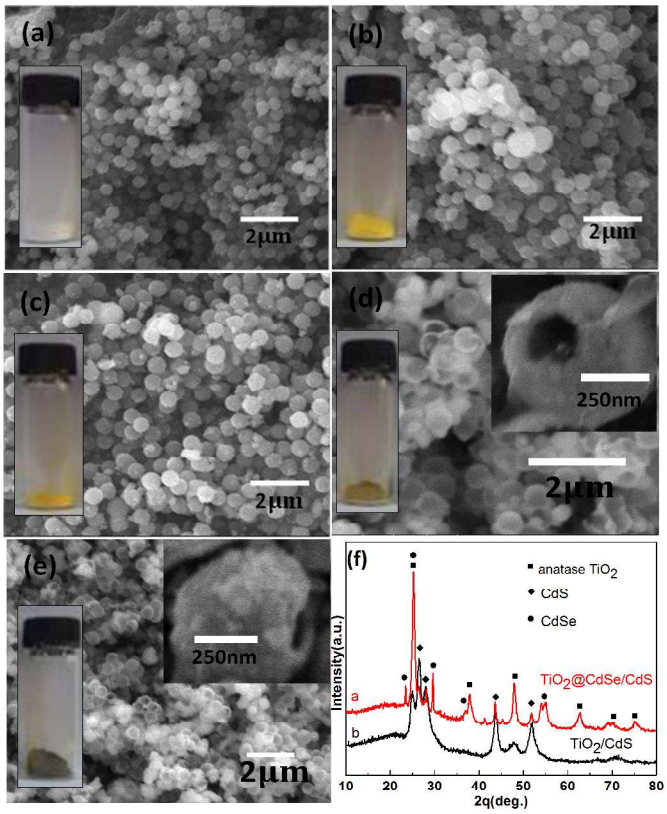

Fig.2. SEM images of the products obtained in each synthesis steps. (a) SiO_2. (b) CdS/SiO_2. (c) TiO_2/CdS/SiO_2. (d) TiO_2/CdS. (e) TiO_2@CdSe/CdS, insets showing an individual nanosphere features. (f) XRD patterns for TiO_2/CdS and TiO_2@CdSe/CdS.

Fig.2 shows the SEM images of the intermediate products obtained at each synthesis step. The digital inserting photograph show an individual nanosphere obtained at synthesis step. Interestingly, the colour change is very obvious between each synthetic step, indicating the formation of different layer. From **Fig.2.a** to **Fig.2.e**, we can see clearly the samples keep sphere shape in the process of synthesis. The average diameters of SiO_2, CdS/SiO_2, TiO_2/CdS/SiO_2, TiO_2/CdS, TiO_2@CdSe/CdS are around 500 nm, 550 nm, 590 nm, 590 nm, 590nm, respectively, indicating that the thicknesses of CdS and TiO_2 layer are both around 40 nm. As can be seen from the inset of **Fig.3.d** and **e**, the broken spheres demonstrate the existence of hollow structures. Hollow spherical THS are uniform with an average diameter of 590 nm. We can also evaluate the thicknesses of the TiO_2/CdS and TiO_2@CdSe/CdS shells is around 90 nm, respectively, which is corresponding to the increase of the thickness during step 2 and step 3. It is also noted that the surface of the TiO2@CdSe/CdS hollow spheres is rougher than that of the TiO_2/CdS. The rough CdSe shell is formed during their refluxed treatment in Selenium source of aqueous solution via ion exchange.

Fig.2.f shows the XRD patterns of TiO_2/CdS (DHS) and TiO_2@CdSe/CdS (THS) samples. Beside the diffraction peaks of anatase TiO_2, diffraction peaks of hexagonal phase CdS and CdSe are also observed, indicating that three-shelled hollow spheres was successfully prepared. The broad diffraction peaks imply that the crystalline grains are on the nanoscale and well-crystallized. The average grain size is estimated according to the Scherrer equation by the full width at half maximum (FWHM) of the diffraction peaks. The average sizes of anatase TiO_2, CdS and CdSe nanocrystals are about 13 nm, 10 nm and 5 nm respectively.

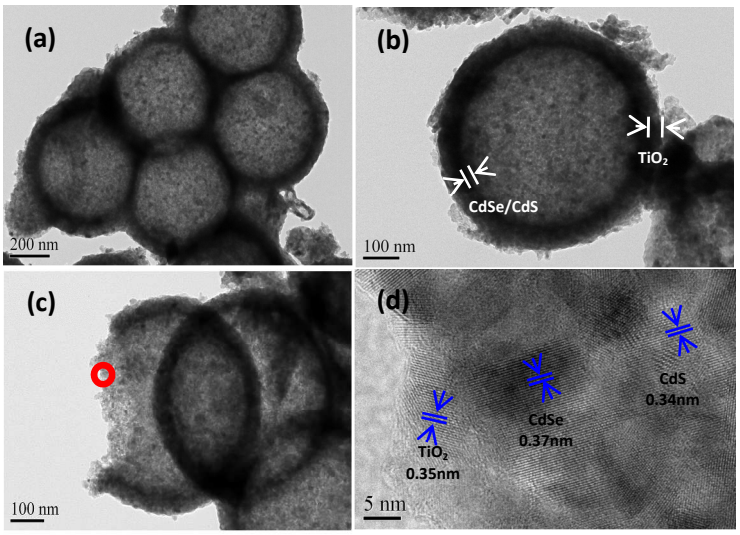

Fig.3. (a-c) TEM images of TiO_2@CdSe/CdS hollow spheres, (d) HRTEM image of the circled area in (c).

To further investigate the material of TiO_2@CdSe/CdS hollow spheres, TEM has been done to characterize the morphology. The TEM images of TiO_2@CdSe/CdS are shown in **Fig.3**. In **Fig.3.a** and b, the hollow spheres are uniformly in the same size, and the diameters of the hollow nanospher can be estimated about 600 nm with a shell thickness of 70 nm. The color contrast between the fringe and central region in **Fig.3.b** confirms the existence of hollow structure. **Fig.3.c** displays a broken hollow sphere, the inner surface could be observed. **Fig.3.d** showed the high resolution transmission electron microscopy (HRTEM) images. The distinct fringes in the HRTEM images provide the identification of the crystallographic spacing of TiO_2, CdSe and CdS nanocrystals. The outboard lattice fringes of 0.35 nm are corresponding to the (101) crystal plane of anatase TiO_2[12]. And the lattice fringes of 0.37 nm and 0.34 nm can be indexed to the (100) of CdSe and (002) of hexagonal CdS[1,30], respectively.

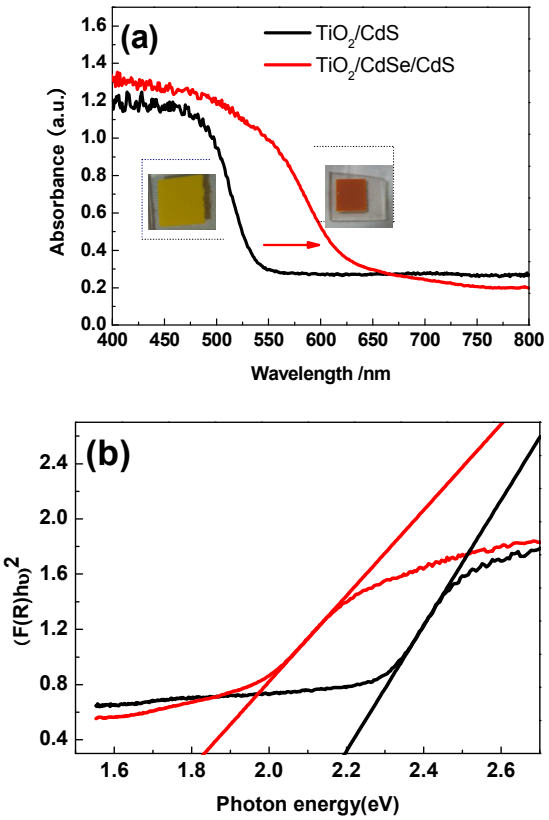

Fig.4. Optical properties of TiO_2/CdS and TiO_2@CdSe/CdSsolar paints, (a) The absorption spectra (b) display of the band gap extraction using Tauc Plot.

We measured the UV−visible absorption spectra of TiO_2/CdS and TiO_2@CdSe/CdS, which are shown in **Fig.4.a**. The absorption spectra can be easily ascribed to the variation of the energy band gaps (Eg) of those two semiconductor sensitizers. Eg for the TiO_2/CdS and TiO_2@CdSe/CdS can be estimated using the conventional Tauc equation by extrapolation of the linear part of the $[F(R)hn]^2$ vs. hn plots[31] (**Fig.4.b**). As we can see, the absorption spectra of the TiO_2/CdS film shows absorption onset around 540 nm, which corresponds to a band gap of 2.2 eV. CdSe exhibits an enhanced light-harvesting effect, after the deposition of CdSe, the absorption edges were expanded observably. TiO_2@CdSe/CdS shows a red-shift in the absorption with onset around 650 nm, which the band gap is 1.8 eV. Just as shown in the **Fig.4.a**, the black-brown colour of TiO_2@CdSe/CdS films further ascertains the ability to capture the incident visible photons. The high absorbance in the visible region reveals the strong absorption properties of the TiO_2@CdSe/CdSsolar paint.

We investigate the solar paint application under heat treatment in the air and N_2 atmosphere. The color has not a very big difference before and after calcination, indicating the outer layer of TiO_2 increased CdSe and CdS thermal stability. The J−V characteristics of these QDSCs are presented in **Fig.5**. The detailed open circuit voltage (Voc), short circuit current (Jsc), fill factor (FF), and power conversion efficiency (Eff) is summarized in **Table 1**.

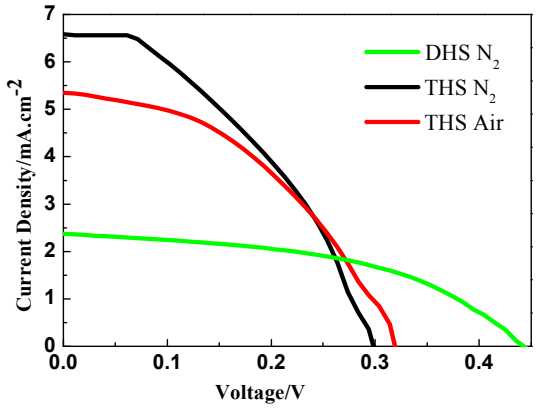

Fig.5. Photocurrent density−voltage (J−V) plot of TiO_2/CdS and TiO_2@CdSe/CdSsolar paints under heat treatment in the air and N_2 atmosphere.

Table 1. The performance of DHS and THS solar paint

	Voc/V	Jsc/ mA/cm2	FF(%)	Eff(%)
DHS N2	0.47	2.38	48	0.54
THS N2	0.30	6.58	42	0.79
THS Air	0.32	5.46	44	0.74

Most striking in **Fig.5**, the current density of THS is as much as twice higher than that of DHS, this may be attributed to CdSe and the novel hollow nanostructure of THS. For the existence of CdSe, on one hand, it increases suction light range of the THS. On the other side, energy level matching of hollow structure can smooth conduction of electrons and holes, thereby increasing the electronic excitation and the cavity electronic separation. For THS, no matter annealing treatment in air atmosphere or in nitrogen atmosphere, there is not much difference, the voltage is higher in the air, while a slightly higher current in nitrogen. This shows the stability of the TiO_2@CdSe/CdS structure in the air.

3. Conclusion

TiO_2@CdSe/CdS hollow spheres were successfully fabricated via hard template and ion exchange route. The diameters of the TiO_2@CdSe/CdS hollow nanospheres were uniformly around 600 nm with a shell thickness of 70 nm. The visible light absorption onset of TiO_2@CdSe/CdS hollow nanospheres is around 650 nm corresponding to a bandgap of 1.8 eV, showing a red-shift when compared with TiO_2/CdS. TiO_2@CdSe/CdS hollow nanospheres can be directly used as solar paint, the photoanode decorated by the solar paint performs a reliable photoelectric conversion efficiency of ~0.79 % with a current density of 6.6 mA/cm^2. The conversion efficiency changed faintly when TiO_2@CdSe/CdS was annealed in N_2 and air atmosphere. This due to the outer layer

of TiO_2 protecting the inner CdSe and CdS from decomposition and increases their stability. Further work is still in progress to convert sun light into electrical energy by using a facile solar paint.

4. Experimental

1. General procedure for synthesis of TiO_2@CdSe/CdS hollow spheres solar paint

Detailed synthesis procedure was depicted as follows:

Step 1.Synthesis of templates SiO_2 nanospheres. SiO_2 nanospheres were synthesized through the decomposition of TEOS along with the right amount of ammonia. To obtain solution A, 5 mL of TEOS was dissolved in 50 mL of ethanol, similarly, to obtain a solution B, 5mL of aqueous ammonia and 10 mL of deionized water were dissolved in 35 mL of ethanol. Mix A and B fully, then the mixed solution vigorously stirred at 40 ℃ for 2.5 h. The precipitate was centrifuged and washed three times with ethanol.

Step 2. Synthesis of CdS/SiO_2 core–shell spheres. CdS/SiO_2 core–shell spheres were fabricated by the ultrasound-driven method. In typically, 0.3 g SiO_2 templates were ultrasonic dispersed in 100 mL of deionized water. 10 mL of the equimolar 0.1 M solution of $CdCl_2$, sodium citrate and thiourea were prepared. The above four kinds of solution were mixed, and the pH value was adjusted to 10.5 by dripping amount of ammonia. The reaction was accomplished under vigorously stirring at 65℃ for 2 h. Then, the precipitate were centrifuged, carefully washed with deionized water and dried in the air.

Step3. Synthesis of TiO_2/CdS/SiO_2 core–shell spheres. 0.3 g prepared CdS/SiO_2 core–shell spheres were ultrasonically dispersed in 150 mL of ethanol to obtain solution A. 3 mL of tetrabutyltitanate (TBT) was dissolved in 50 mL of ethanol to obtain solution B. Solution B and 1.5 mL of aqueous ammonia were added to solution A, vigorously stirred at 60 ℃ for 3 h. The precipitate TiO_2/CdS/SiO_2 core–shell spheres were centrifuged, carefully washed with ethanol and dried in air. Then, they were annealed at 550 ℃ for 1 h in air to crystallize TiO_2.

Step 4. Synthesis of TiO_2@CdSe/CdS solar paint. TiO_2/CdS/SiO_2 core–shell spheres were placed in the 80 mL Teflon-lined autoclave filled to 80 % capacity with 1 M NaOH and the sealed autoclave was placed in the 80℃oven for 4 h. The autoclave was then cooled naturally to room temperature. Finally, the TiO_2/CdS was washed several times with distilled water. CdSe shell is structured by the ion exchange method. Briefly, 0.4 g of Se, 0.8 g of Na_2SO_3, 0.3 g of TiO_2/CdS (DHS) and 20 mL of deionized water were refluxed for 7 h under constant stirring until the solution becomes dark brown. The TiO_2@CdSe/CdShollow spheres were centrifuged and carefully washed with deionized water and dried in air.

2. Preparation of Solar Paint and Cell Construction

TiO_2@CdSe/CdSshell spheres were printed on a transparent conductive FTO (fluorine-doped tin oxide, 14 Ω per square, Nippon Sheet Glass, Japan) glass after dispersed in the ethanol solution containing ethyl cellulose and terpineol, followed by sintering process at 450 ℃ for 30 minutes in the air or in N_2 atmosphere, respectively. The solar cells were assembled into sandwich-type device by separating the counter electrode and the photoanode with a hot-melt gasket (25μm, Surlyn1702, DuPont). The counter electrode hired a Cu_2S, the construction of which is described elsewhere[19]. A mixture of 1M sodium sulfide and 1M sulfur was employed as the electrolyte.

3. Characterization

The morphology observations were examined by scanning electron microscope (SEM, FEI, Quanta-200) and Field Emission scanning electron microscopy (FESEM, HITACHI S-4800). The high-resolution transmission electron microscopy (HR-TEM) investigation was carried out on a JEM-2010UHR instrument (JEOL, Japan), using an acceleration voltage of 200kV. X-ray powder diffraction (XRD) data was collected by a Rigaku Smart Lab automatic diffractometer, with Cu-Kα radiation (λ=1.541Å)at 40kV and 40mA. The XRD patterns were recorded with a scanning increment of 0.05° at a scan speed of 0.02° second/step in the range of 10°-80°(2θ degree). The UV-vis diffuse reflectance spectra obtained of the as prepared TiO_2@CdSe/CdS films were measured by by a UV-Vis spectrophotometer (Persee, China).The I-V characteristics of the solar cells were measured employing a Newport oriel solar simulator (model 94023A-450W) and Keithley 2420 source meter (USA) under simulated solar light (AM 1.5 G, 100 $mW.cm^{-2}$) which was calibrated with a standard silicon solar cell equipped with a filter. The active area of PSSC utilized in the I-V test was 0.16 cm^2.

Acknowledgements

This research was supported by the Natural Science Foundation of China (No. U1162108, No. 51272104); the Natural Science Foundation of Jiangsu Province Office of Education (No.11KJA150002; No.10KJB150006), the Financial Foundation of State Key Laboratory of Materials-Oriented Chemical Engineering and A Project Funded by the Priority Academic Program Development of Jiangsu Higher Education Institutions.

Notes and references

Address. State Key Laboratory of Materials-Oriented Chemical Engineering, College of Chemistry and Chemical Engineering, Nanjing University of Technology, Nanjing, 210009, China

1. R. S. Selinsky, Q. Ding, M. S. Faber, J. C. Wright and S. jin, *Chem. Soc. Rev.*, 2013,**42**,2963.
2. Z. Yang, C. Y. Chen, P. Roy and H.T. Chang, *Chem. Commun.*, 2011, **47**,9561.
3. I. Morasero, S. Gimenez, F. S. Francisco Q. Shen and J. Bisquert, *Acc. Chem. Res.*, 2009,**42**,1848.
4. M. Shalom, Z. Tachan, Y. Bouhadana, H. N. Barad and A. Zaban, *J. Phys. Chem. Lett.*, 2011,**2**,1998.

5. A. J. Nozik, *Physica E*, 2002,**14**,115.
6. J. T. Margraf, A. Ruland, V. sgobba, D. M. Guldi and T.Clark, *Langmuir*, 2013,**29**,2434.
7. M. Shalom, S. Buhbut, S. Tirosh and A. Zaban, *J. Phys. Chem. Lett.*, 2012,**3**, 2436.
8. J. Yang, L. K. Pan, G. Zhu, X. J. Liu, H. C. Sun and Z. Sun, *J. Electroanal. Chem.*, 2012,**677**,101.
9. J. Li, L. Zhao, S. M. Zhao, J.H. Hu, B. H. Dong and H.B.Hu, *Mater. Res. Bull.*, 2013,**48**,2566.
10. S. Kim, S. H. Im, M. Kang, J. H. Heo, S. I. Seok, S. W. Kim and I. Mora, *Phys. Chem. Chem. Phys.*, 2012,**14**, 14999.
11. K. Shin, J. B. Yoo and J. H. Park, *J. Power Sources*, 2013,**225**, 263.
12. G. Zhu, L. K. Pan, T. Xu and Z. Sun, *Appl. Mater. Interfaces*, 2011,**3**,3146.
13. L. C. Chen, Y. C. Ho, R. Y. Yang, J. H. Chen and C. M. Huang, *Appl. Surf. Sci.*, 2012, **258**,6558.
14. J. Li, C. J. Lin, J. T. Li and Z. Q. Lin, *Thin Solid Films*, 2011,**519**,5494.
15. C. H. Chang and Y. L. Lee, *Appl. Phys. Lett.*, 2007,**91**, 535.
16. Y. L. Lee and C. H. Chang, *J. Power Sources*, 2008,**185**,584.
17. N. Biswal, and K. M. Parida, Int. *J. Hydrogen Energy*, 2013,**38**,1267.
18. H. M. Chen, C. K. Chen, C. C. Lin, R. S. Liu, H. Yang, W. S. Chang, K. H. Chen, T. S. Chan, J. F. Lee and D. P. Tsai, *J.Phys. Chem. C*, 2011,**115**, 21971.
19. J. W Lee, D. Y. Son, T. K. Ahn, H. W. Shin, I. Y. Kim, S. J. Hwang and N. G. Park, *Sci. Rep.*, 2013, **3**, 1050.
20. Y. L Lee, and Y. S. Lo, *Adv. Funct. Mater.*, 2009, **19**,604.
21. Z. H. Chen, S. Y. Yeung, H. Li, J. C. Qian, W. J. Zhang, Y. Y. Li and I. Bello, *Nanoscale*, 2012, **4**,3154.
22. P. Yu, K. Zhu, A. G. Norman, S. Ferrere, A. J. Frank and A. J. Nozik, *J. Phys. Chem. B*, 2006,110.
23. Z. X. Li, Y. L. Xie, H. Xu, T. M. Wang. G. Xu and H. L. Zhang, *J. Photochem. Photobiol. A*, 2011, **224**, 25.
24. J. Yan, Q. Ye, and F. Zhou, *Adv. Mater.*, 2012,**2**,3978.
25. E. H. Kong, Y. J. Chang,Y. C. Park, Y. H. Yoon, H. J. Park and H. M. Jang, Phys. *Chem. Chem. Phys*., 2012,**14**, 4620.
26. Y. K. Lai, Z. Q. Lin, D. J. Zheng, L. F. Chi, R. G. Du and C. J. Lin , *Electrochim. Acta*, 2012,**79**,175.
27. C. H. Li, L. Yang, J. Y. Xiao, Y. C. Wu and M. Sondergaard, *Phys. Chem. Chem. Phys*, 2013,**15**, 8710.
28.T. Toyoda, k. Oshikane, D. M. Li, Y. H. Luo, Q. B. Meng and Q. Shen, *J. Appl. Phys.*, 2010,**108**, 114304.
29. Z. Zhu, J. H. Qiu, K. Y. Yan and S. H. Yang, *Appl. Mater. Interfaces*, 2013,**5**,4000.
30. P. K. Santra and P. V . Kamat, *J. Am. Chem. Soc.*, 2012, **134**, 2508.
31. J. J. Tian, Q. F. Zhang, L. L. Zhang and R. Gao, *Nanoscale*, 2013, **5**, 936.
32. Z. X. Pan, H. Zhou, K. Cheng, Y. Hou, J. Hua and X. Zhong, *ACS Nano*, 2012,3982.